Monthly Notices
of the
ROYAL ASTRONOMICAL SOCIETY

MNRAS **466,** 2143–2150 (2017)
Advance Access publication 2016 December 14

doi:10.1093/mnras/stw3236

Luminosity dependence of the cyclotron line and evidence for the accretion regime transition in V 0332+53

Victor Doroshenko,[1]★ Sergey S. Tsygankov,[2] Alexander A. Mushtukov,[3,4] Alexander A. Lutovinov,[5,6] Andrea Santangelo,[1] Valery F. Suleimanov[1] and Juri Poutanen[2,7]

[1]*IAAT, University of Tuebingen, Sand 1, Tuebingen D-72076, Germany*
[2]*Tuorla Observatory, Department of Physics and Astronomy, University of Turku, Väisäläntie 20, FI-21500 Piikkiö, Finland*
[3]*Anton Pannekoek Institute, University of Amsterdam, Science Park 904, NL-1098 XH Amsterdam, the Netherlands*
[4]*Pulkovo Observatory of the Russian Academy of Sciences, Saint Petersburg 196140, Russia*
[5]*Space Research Institute of the Russian Academy of Sciences, Profsoyuznaya Str. 84/32, Moscow 117997, Russia*
[6]*Moscow Institute of Physics and Technology, Moscow region, Dolgoprudnyi, 117303, Russia*
[7]*Nordita, KTH Royal Institute of Technology and Stockholm University, Roslagstullsbacken 23, SE-10691 Stockholm, Sweden*

Accepted 2016 December 9. Received 2016 December 6; in original form 2016 April 29

ABSTRACT

We report on the analysis of *NuSTAR* observations of the Be-transient X-ray pulsar V 0332+53 during the giant outburst in 2015 and another minor outburst in 2016. We confirm the cyclotron-line energy–luminosity correlation previously reported in the source and the line energy decrease during the giant outburst. Based on 2016 observations, we find that a year later the line energy has increased again essentially reaching the pre-outburst values. We discuss this behaviour and conclude that it is likely caused by a change of the emission region geometry rather than previously suggested accretion-induced decay of the neutron stars magnetic field. At lower luminosities, we find for the first time a hint of departure from the anticorrelation of line energy with flux, which we interpret as a transition from super- to sub-critical accretion associated with the disappearance of the accretion column. Finally, we confirm and briefly discuss the orbital modulation observed in the outburst light curve of the source.

Key words: X-rays: binaries – X-rays: individual: V 0332+53.

1 INTRODUCTION

In binary systems, the accretion of matter supplied by a non-degenerate companion on to a strongly magnetized ($B \sim 10^{12}$ G) rotating neutron star (NS) results into pulsed X-ray emission from the vicinity of NS magnetic poles. The plasma is channeled to the polar caps by the magnetic field of the NS, which also has a profound effect on the observed X-ray spectra. In particular, the motion of the electrons in a strong magnetic field is quantized, which gives rise to the so-called cyclotron resonance scattering features (CRSFs; see Mushtukov, Nagirner & Poutanen 2016 for a recent review). A single (fundamental) or multiple harmonics (Santangelo et al. 1999) absorption-like features can be observed in the X-ray band depending on the conditions in the line-forming region. In particular, the energy of the fundamental is related to the magnetic field strength as $E_{\rm cycl} \sim 12\,{\rm keV}\,B/10^{12}$ G.

The structure of the emission region in the vicinity of the NS and thus the origin of the CRSF are, however, uncertain. At low accretion rates, most of the observed emission likely comes directly from the accretion mounds on the polar caps of the NS, where the gravitational energy of the flow is released. However, the observed luminosities of bright pulsars by far exceed the local Eddington limit for kilometre-sized polar caps. At high accretion rates, the plasma must be, therefore, stopped above the NS surface by the radiative pressure, and the observed emission has to emerge from the extended 'accretion column' (Basko & Sunyaev 1976; Becker et al. 2012; Mushtukov et al. 2015b). Conditions for the transition between the two regimes are determined by the largely unknown geometry of the column, and by the angular- and energy-dependent plasma opacities, which makes it extremely hard to make robust theoretical predictions on the transition (critical) luminosity (Mushtukov et al. 2015a, b).

On the other hand, analysis of the luminosity dependence of the observed properties of X-ray pulsars might help to constrain the critical luminosity observationally (Tsygankov et al. 2006; Staubert et al. 2007; Klochkov et al. 2012). Indeed, in low luminous sources, the CRSF energy typically increases with the flux, whereas at higher accretion rates, an anticorrelation is observed. As discussed by Staubert et al. (2007), Becker et al. (2012), Mushtukov et al. (2015a)

★ E-mail: doroshv@astro.uni-tuebingen.de

Table 1. Observation log and best-fitting results for the phase-averaged spectrum using the `CompTT` model. For *INTEGRAL*/SPI, some of the parameters (shown in italic) were fixed to values derived from *NuSTAR* data at closest luminosity level. Luminosity is calculated based on the observed flux in the 3–80 keV band not accounting for interstellar absorption or the CRSFs, and assuming a distance of 7 kpc.

Observation ID	Date (MJD)	Exposure (ks)	$E_{\rm cycl}$ (keV)	$\sigma_{\rm cycl}$ (keV)	$D_{\rm cycl}$	T_0 (keV)	kT_e (keV)	τ	L_{37}, 3–80 keV 10^{37} erg s^{-1}	χ^2/dof
80102002002	57223	10.5	27.93(2)	8.47(8)	0.863(2)	1.40(1)	5.85(4)	16.4(1)	16.04	0.97/2864
80102002004	57276	14.9	28.25(2)	7.59(8)	0.861(2)	1.19(1)	5.73(5)	18.3(1)	7.98	0.9/2628
80102002006	57282	17.3	28.40(2)	7.43(8)	0.862(2)	1.03(2)	5.76(5)	19.7(1)	5.45	0.84/2600
80102002008	57296	18.2	29.03(4)	6.73(8)	0.899(3)	0.78(3)	6.08(5)	18.5(1)	1.71	0.88/1724
80102002010	57300	20.1	28.90(5)	6.30(1)	0.895(4)	0.73(5)	6.09(7)	17.7(1)	0.91	0.83/1375
90202031002	57599.8	25.2	30.42(5)	6.80(1)	0.925(4)	0.66(5)	6.80(1)	16.5(1)	0.57	0.88/1369
90202031004	57600.8	25.0	30.28(6)	6.90(1)	0.921(4)	0.68(5)	6.90(1)	16.4(1)	0.46	0.91/1330
rev. 1565	57220	67.8	28.28(7)	*8.47*	0.845(5)	*1.4*	*5.85*	*16.4*	∼19.5	0.89/110
rev. 1570	57233	141	27.64(5)	*8.47*	0.814(4)	*1.4*	*5.85*	*16.4*	∼23.1	1.2/110
rev. 1596	57302	120	29(2)	*6.30*	0.4(3)	*0.73*	*6.1*	*17.7*	∼1.0	0.88/10

and Mushtukov et al. (2015c), this behaviour could point to the two accretion regimes corresponding to sub- and super-critical accretion. Observing the transition between the two regimes in a single source would strongly support this interpretation. In this paper, we report on the analysis of the CRSF luminosity dependence in the Be-transient X-ray pulsar V 0332+53 during the giant outburst in 2015 and another minor outburst in 2016, and discuss the complex evolution of the line energy throughout the giant outburst and between the two outbursts, which, we argue, provides the first evidence for such transition.

2 OBSERVATIONS AND DATA ANALYSIS

We focus on the analysis of five dedicated *NuSTAR* observations during the 2015 giant outburst aimed to detect the transition from the super- to sub-critical accretion regime. We verify the *NuSTAR* results using the *INTEGRAL*/SPI observations of the source during the outburst (*INTEGRAL* revolutions 1565, 1570 and 1596). Additionally, we report on two follow-up *NuSTAR* observations obtained in 2016 July during another periastron passage aimed to extend the observational coverage at low luminosities. We note that the source flux in the last two observations approaches that for the transition of the source to propeller (Tsygankov et al. 2016), so we probe here the lowest fluxes when the source is still accreting. The observation log is presented in Table 1 and Figs 1 and 2. Finally, we used also *Swift*/XRT data contemporary to the *NuSTAR* observations to extend the low-energy band and monitor the activity of the source near the periastron passage in 2016 July.

The *NuSTAR* data reduction was carried out using the HEASOFT 6.19 package with current calibration files (CALDB version 20160824) and standard data reduction procedures as described in the instruments documentation. Source spectra were extracted from a region of 120 arcsec radius around V 0332+53. The background spectra were extracted from a circular region of 80 arcsec radius as far away from the source as possible for each observation. The spectra for the two *NuSTAR* units were extracted and fitted simultaneously between 5 and 79 keV for the outburst observations (Fürst et al. 2013), and in 3–79 keV range for the last two observations, where no *Swift* data were available. To extract the *Swift*/XRT spectra, we used the *Swift* data products service provided by the UK Swift Science Data Centre,[1] as described in Evans et al. (2009). All *NuSTAR*/*Swift* spectra were grouped to at least 25 counts per bin and fitted using the XSPEC version 12.9 with Gehrels weighting (Gehrels 1986).

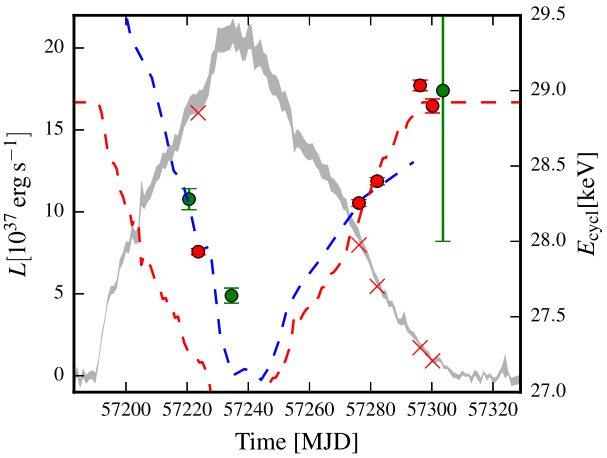

Figure 1. *Swift*/BAT light curve in the 15–50 keV band (grey) of V 0332+53 during the 2015 giant outburst scaled to match the source luminosity measured using *NuSTAR* pointed observations (red crosses). The red and green circles with error bars indicate the CRSF fundamental energy as measured by *NuSTAR* and *INTEGRAL*/SPI, respectively. The red dashed line shows the model prediction for the fundamental energy based on the CRSF energy versus luminosity correlation measured by *NuSTAR* in the declining part of the outburst. The blue dashed line shows the fundamental energy reported by Cusumano et al. (2016) shifted by 1 keV. The shift is likely due to the difference in absolute energy scale of *Swift*/BAT with respect to *NuSTAR* and SPI.

INTEGRAL observed V 0332+53 four times during the spacecraft revolutions 1565, 1570, 1586 and 1596. Problems with the energy calibration of IBIS and JEM-X telescopes did not permit us to reconstruct the source spectrum properly. However, we were able to do it for three observations where the SPI spectrometer was operating (detectors annealing was performed during revolution 1586). The *INTEGRAL*/SPI data were screened and reduced in accordance with the procedures described by Churazov et al. (2011, 2014).

The broad-band spectrum of the source has been previously described (Tsygankov et al. 2006; Lutovinov et al. 2015) using a power law with cutoff at high energies (`CUTOFFPL` model in XSPEC) modified by interstellar absorption and one-to-three broad absorption features accounting for the CRSF at ∼26 keV and its harmonics at ∼50 and ∼72 keV (Tsygankov et al. 2006). To account for the CRSF and the first harmonic, we use the multiplicative Gaussian $G(E) = 1 - D_{\rm cycl} {\rm e}^{-\ln 2((E-E_{\rm cycl})/\sigma_{\rm cycl})^2}$ rather than the

[1] http://www.swift.ac.uk/user_objects/

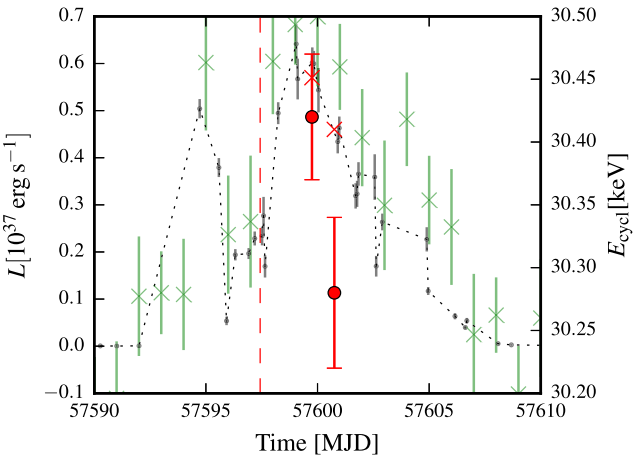

Figure 2. *Swift*/XRT (0.3–10 keV, grey points with error bars) and *Swift*/BAT (15–50 keV, green crosses with error bars) light curves of V 0332+53 during the 2016 August periastron passage scaled to match the source luminosity measured using *NuSTAR* pointed observations (red crosses). The red error bars indicate the CRSF fundamental energy as measured by *NuSTAR*.

exponential Gaussian (GABS in XSPEC), or the pseudo-Lorentzian model (CYCLABS in XSPEC) used by Tsygankov et al. (2006). Indeed, the latter model was designed to mimic the high energy cutoff (Mihara et al. 1990), which is already included in the continuum model. As a consequence, the measured line centroid E_0 becomes coupled to the cutoff energy and shifted by σ^2/E_0 with respect to the true centroid (Nakajima, Mihara & Makishima 2010), which complicates the interpretation of the results. On the other hand, the exponential Gaussian profile usually used to describe the CRSFs yields a slightly worse fit with systematic ∼1–2 per cent residuals around the line, especially for the CUTOFFPL continuum. This behaviour has been reported by Pottschmidt et al. (2005) and Nakajima et al. (2010) for the 2005 outburst and was interpreted as evidence for a complex CRSF profile. We find, however, that the magnitude of the residuals depends on the continuum model used (for instance, they essentially disappear for the HIGHECUT model). Furthermore, restricting the energy range to 20–80 keV as well as using a multiplicative Gaussian or Lorentzian line profile results in no significant residuals for any continuum model. We conclude, therefore, that given the existing uncertainties in the modelling of the broad-band continuum of X-ray pulsars, there is no strong evidence for a more complex line profile in *NuSTAR* data. This conclusion is consistent with *Swift*/BAT results (Cusumano et al. 2016), where the Gaussian line provided an adequate description of the data.

We verified that the measured CRSF centroid does not depend on the continuum or line model used and is well constrained for all *NuSTAR* observations. In particular, we measured consistent CRSF energies (within the uncertainties) using the broad-band fits of *NuSTAR* + *Swift*/XRT data and HIGHECUT or a comptotnization model CompTT by Titarchuk (1994), as well as for *NuSTAR* data in the 20–80 keV range and the CUTOFFPL model for either Lorentzian and Gaussian line profiles. In all cases, an inclusion of the additional soft blackbody component with a temperature of ∼0.4 keV improves the fit for the XRT data, although, taking into account large systematic uncertainties in the window-timing mode, it is unclear whether this component is real. For all models, we also accounted for interstellar absorption. It was sufficient to assume the absorption column fixed to the average value of 2×10^{22} cm^{-2} for all observations. We note that the absorption column is similar to the one derived from XRT observations in later phases of the outburst (Tsygankov et al. 2016), so there is no evidence for enhanced absorption during the bright phase of the outburst. Neither component significantly affects the derived CRSF parameters. The CompTT continuum model provides, however, the most stable and consistent fit for all observations; therefore, we use this model combined with the Gaussian profile for the CRSF for the rest of analysis. On the other hand, *INTEGRAL* data do not allow us to reliably constrain the continuum, so we fix respective parameters to the values derived from the *NuSTAR* data at closest luminosity and only fit for the CRSF parameters. Again, we have verified that the derived line parameters are not significantly affected by the choice of the continuum model also in this case. We also found that at low fluxes the width of the first harmonics becomes poorly constrained due to the correlation with continuum temperature. We assumed, therefore, that the relative width of the harmonic (i.e. $\sigma_{\rm cycl,1}/E_{\rm cycl,1} = \sigma_{\rm cycl}/E_{\rm cycl}$) is the same at all luminosities. In spectra with the highest statistical quality, the second harmonic becomes visible in the residuals, although not really significant. This is not surprising as *NuSTAR* is sensitive only up to 78 keV, so we did not include the second harmonic in the model. The results of the fits are presented in Table. 1. Unfolded spectra for the best-fitting model and respective residuals are shown in Fig. 3. All uncertainties are quoted at a 1σ confidence level and include no systematic error, unless stated otherwise.

It is interesting to note that there is an apparent shift by ∼1 keV between *NuSTAR* and *INTEGRAL* data (which are consistent with each other) and the *Swift*/BAT measurements reported by Cusumano et al. (2016), as illustrated in Fig. 4. This mismatch is probably related to the difference in absolute energy calibration between the instruments as *INTEGRAL* measurements are also consistent for the current and previous outbursts (Ferrigno et al. 2016). Besides this shift, the difference in absolute flux calibration of the instruments and difference in energy ranges used to calculate luminosities need to be taken into account for a direct comparison of the results. In particular, we recalculated the *Swift*/BAT luminosities reported by Cusumano et al. (2016) using the *Swift*/BAT 15–50 keV light curve and contemporary *NuSTAR* fluxes, which turn out to be well correlated. Based on this correlation, we estimate the $L_{\rm x} = 91(2)C(10^{37}$ erg s$^{-1})$ conversion factor (here C is the observed BAT count rate). Once said corrections are taken into account, the CRSF energies measured by all three observatories become compatible within uncertainties, as illustrated in Fig. 4.

We also carried out the pulse-phase-resolved analysis of all *NuSTAR* observations. The complex spin frequency evolution (Doroshenko, Tsygankov & Santangelo 2016) and long intervals between the individual observations prevented us from obtaining a single phase-coherent timing solution. Therefore, we phased all observations using the reference epochs obtained through fitting the CRSF energy pulse profile with a cosine function. The corresponding pulse profiles in the 3–15 and 15–80 keV energy bands are also plotted for reference in Fig. 6. For the phase-resolved analysis, we additionally fixed the CompTT temperatures and iron line parameters to average values.

3 DISCUSSION

3.1 CRSF centroid energy drift

The source is known to exhibit an anticorrelation of the CRSF centroid energy with luminosity, which is believed to be caused by a change of the accretion column height and was studied extensively during the 2004–2005 outburst (Tsygankov et al. 2006;

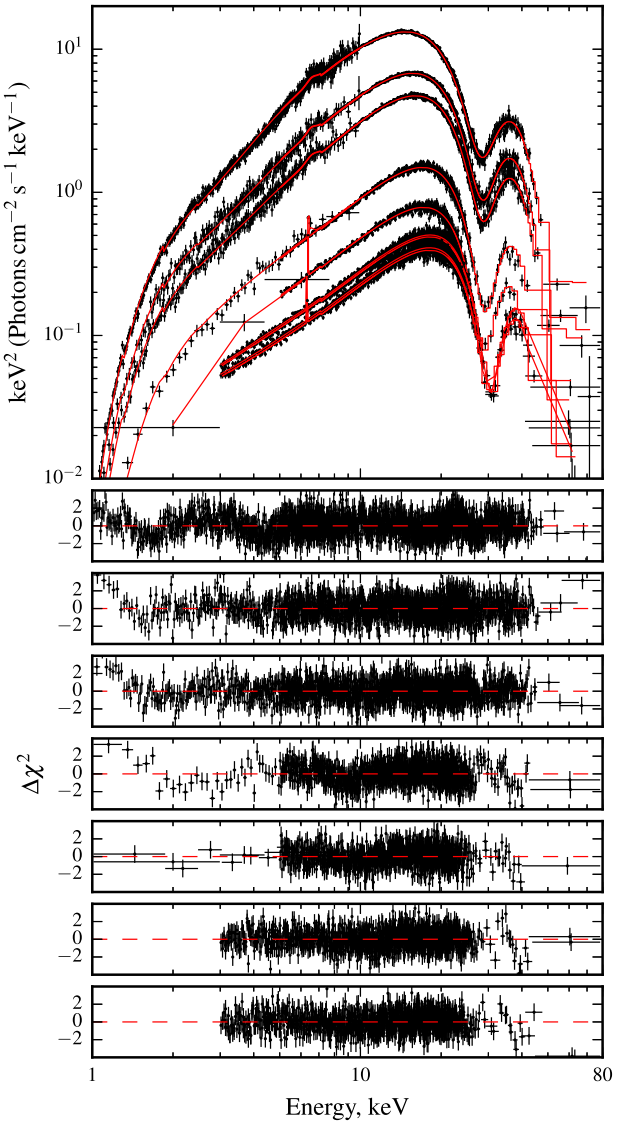

Figure 3. Unfolded spectra as observed by *NuSTAR* (5–80 keV) and *Swift*/XRT (1–10 keV), and the corresponding best-fitting residuals for the brightest to the dimmest observations (top to bottom, top panel).

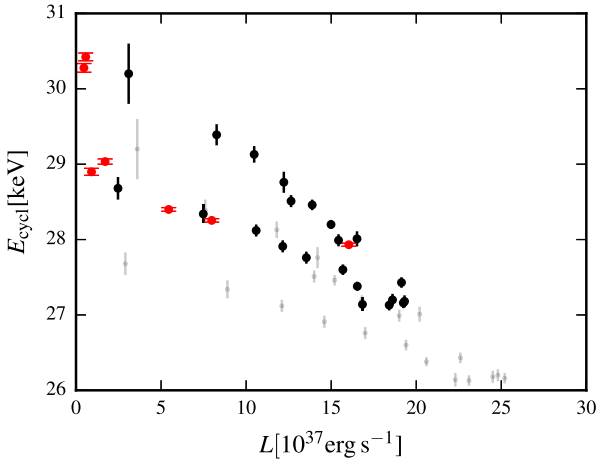

Figure 4. Dependence of the fundamental centroid energy on luminosity, as observed by *NuSTAR* in 2015–2016 (red points). The same correlation as reported by Cusumano et al. (2016) based on *Swift*/BAT data is also plotted for reference (grey points). Note that the assumed spectral model and energy range used to calculate the luminosity were different in the two cases (see text). The apparent ∼1 keV shift between the two instruments is likely related to the difference in their absolute energy calibration. Once this shift and correction to the luminosity are taken into account, the agreement between *Swift* and other instruments becomes acceptable (black points).

Tsygankov, Lutovinov & Serber 2010; Poutanen et al. 2013; Lutovinov et al. 2015). The *NuSTAR*, *INTEGRAL* and *Swift* observations reveal a similar behaviour for the current outburst, although with two important differences. First, line energies measured during the declining part of the outburst seem to be significantly lower for comparable luminosity levels (Cusumano et al. 2016), which was not the case in 2005 (Tsygankov et al. 2010). The reported drop of the centroid energy reaches ∼1.5 keV for *Swift*/BAT data (the blue dashed line in Fig. 1). This is fully consistent with our *NuSTAR* and *INTEGRAL* results, as shown in Figs 1 and 4. Note that the two *NuSTAR* observations in 2016 July reveal, for the first time, that after the ∼1.5 keV drop during the 2015 outburst the centroid energy has again increased by the same amount effectively negating the observed decay during the outburst.

Cusumano et al. (2016) argued that the observed decrease of the CRSF energy is due to the screening of the NS dipole magnetic field by the accreting matter. The efficiency of this mechanism depends on the ratio of time-scales for field 'burial' through the advection by accreting matter and re-emerging of the field driven by magnetic buoyancy, Ohmic diffusion or other mechanisms (Choudhuri & Konar 2002). While both time-scales are highly uncertain, it is still interesting to compare V 0332+53 with other sources where a variation of the CRSF energy with time has been reported. The net decay rate of the CRSF during the outburst is $\dot{E}_{\rm cycl} \sim 1.5\,{\rm keV}/100\,{\rm d}$, and the net increase rate between the outbursts at least $\dot{E}_{\rm cycl} \sim 1.5\,{\rm keV}/300\,{\rm d}$. If accretion is, indeed, responsible for the screening of the magnetic field, the field-increase rate shall remain the same also in the outburst, so the advection shall reduce the field even faster than observed. The corresponding field decay/re-emerging time-scales $\tau = E_{\rm cycl}/\dot{E}_{\rm cycl} \sim 4{-}16$ yr turn out to be significantly shorter than observed for other sources and generally expected from a theoretical point of view. For instance, in Vela X−1 and Her X−1, the CRSF decay rates of $\sim -9.7 \times 10^{-4}$ (La Parola et al. 2016) and $\sim -7 \times 10^{-4}$ keV d^{-1} (Klochkov et al. 2015; Staubert et al. 2016) imply $\tau \sim 70$–155 yr.

Another issue with this interpretation is related to the spin evolution of V 0332+53 during the outburst, which is governed by a balance of the accelerating and braking torques exerted on to the NS (Rappaport & Joss 1977; Ghosh & Lamb 1979; Lipunov, Semenov & Shakura 1981; Lipunov 1982a; Wang 1987). While both torques increase with the magnetosphere size, the braking torque is more sensitive to the field strength and thus shall decrease faster than the accelerating torque if the intrinsic field of the NS, indeed, drops by ∼5 per cent, as suggested by Cusumano et al. (2016). One can, therefore, expect the net spin-up rate of the NS to increase during the declining phase of the outburst. However, the opposite is observed, as reported by Doroshenko et al. (2016) and illustrated in Fig. 5. The observed spin-up rate actually decreases for a given accretion rate during the later phases of the outburst, which implies ∼30 per cent increase of the magnetic field strength [assuming the torque model by Lipunov (1982b) and the $B = 3.4 \times 10^{12}$ G field for the rising phase of the outburst, as deduced from the observed CRSF energy; however, a similar result can be obtained for the Ghosh & Lamb (1979) model]. We conclude, therefore, that the spin evolution of the source is inconsistent with the intrinsic field

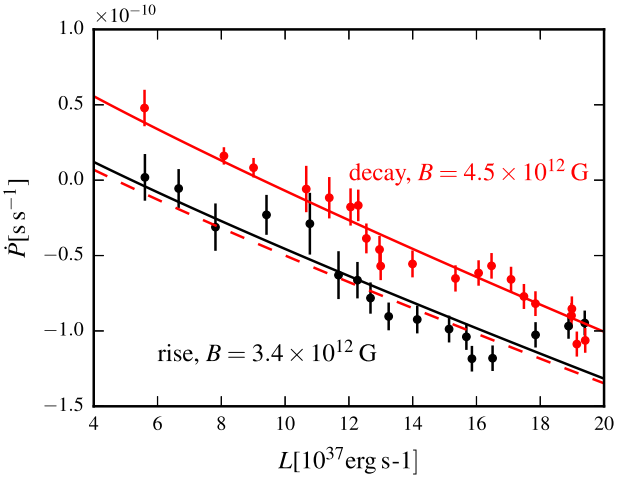

Figure 5. Correlation of the spin-up rate with flux, as reported in Doroshenko et al. (2016). A best-fitting prediction for the torque model by Lipunov (1982b) with $B = 3.4 \times 10^{12}$ G and $B \sim 4.5 \times 10^{12}$ G for rising (black) and declining (red) parts of the outburst, respectively, is also shown for reference. An ∼5 per cent magnetic field decay suggested by Cusumano et al. (2016) would imply a slightly higher spin-up rate for the declining part of the outburst (with respect to the rising part), as indicated with the red dashed line.

decay suggested by Cusumano et al. (2016) and must be related to other factors. A detailed discussion of this issue is out of scope for this work, and we can only speculate that the observed change of the spin-up rate might be associated with the viscous evolution of the accretion disc during the outburst. Indeed, the disc is expected to have a higher surface density and thus might push further into the magnetosphere during the rising phase of the outburst, which would imply a lower magnetospheric radius (for the same field strength of the NS) and thus a higher spin-up rate. We note that a comparable total amount of accreted mass during the 2005 and 2015 outbursts (Cusumano et al. 2016) together with a significantly longer duration of the later outburst suggests that the accretion disc did, indeed, have different structures in the two cases.

So what besides the decay of intrinsic magnetic field could cause the observed CRSF energy decrease? We note that the magnitude of the line energy drop is comparable with the variation of line energy with pulse phase (see Fig. 6) and luminosity, so it is natural to attribute the observed CRSF decay to a change in the geometrical configuration of the line-forming region. Such change can be caused by several factors besides the variation of the NS intrinsic field, for instance, by a change of the effective magnetospheric radius, which, as discussed above, is also suggested by the spin evolution of the pulsar. In the context of the model by Poutanen et al. (2013), the CRSF is formed via a reflection of beamed radiation from the accretion column off the unevenly illuminated NS atmosphere, so the observed change in CRSF energy corresponds to a change of the illumination pattern. The footprint of the accretion column is expected to be reduced for larger magnetospheric radii as the plasma follows the field lines that are closer to the magnetic pole in this case. Decrease of the footprint implies that the accretion column becomes taller for a given luminosity and thus more effectively illuminates equatorial regions of the NS, resulting in a lower observed CRSF energy, as illustrated schematically in Fig. 7.

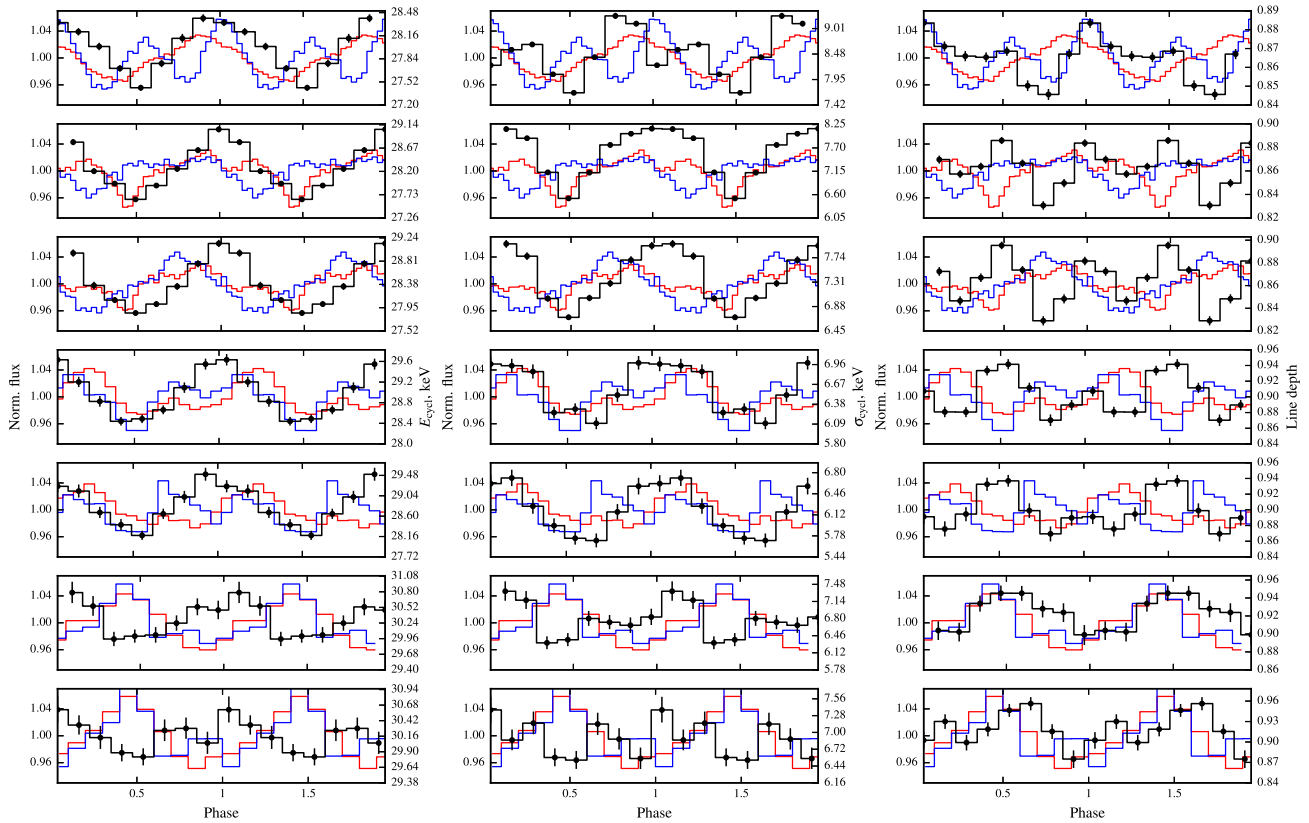

Figure 6. Pulse phase dependence of the CRSF energy as observed by *NuSTAR* (black histogram) at different luminosities ($L/10^{37}$ erg s^{-1} = 16.04, 7.98, 5.45, 1.71, 0.91, 0.57 and 0.46, top to bottom). The pulse profiles in the 3–15 and 15–80 keV ranges (blue and red steps) are also shown. The pulse phase of individual observations was aligned so that zero phase corresponds to maximal CRSF energy.

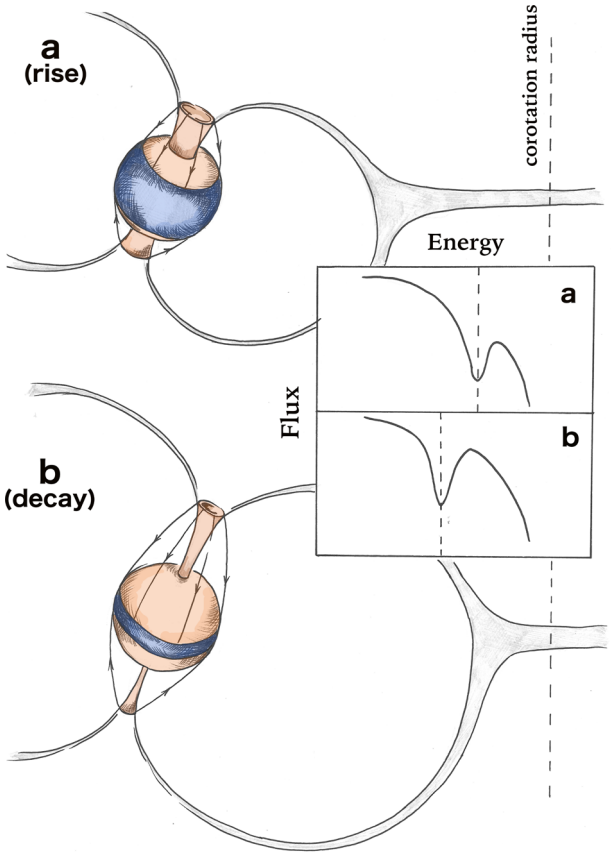

Figure 7. Change of the accretion disc structure and of the magnetospheric radius (with respect to the corotation radius indicated by the vertical line) changes both the net torque exerted on to the NS and the accretion column height. During the declining phase, the matter falls closer to the polar areas, which increases the height of the accretion column so that the illumination pattern shifts to the equatorial areas, implying a lower observed CRSF energy.

Changes in the emission region geometry must be reflected in the pulse profile shape. Indeed, the pulse profiles observed at comparable luminosities in the declining phase of the 2015 outburst and in 2016 do appear to be significantly different, as illustrated in Fig. 6. On the other hand, in the context of the reflection model, almost the entire NS surface is illuminated in both cases, so no drastic changes for the phase dependence of the CRSF parameters are expected, which is again qualitatively consistent with the results of phase-resolved analysis. An additional argument supporting the proposed interpretation comes from the comparison of the relative amplitude of the CRSF energy variation with pulse phase in different observations. This turns out to be significantly higher for observations in the declining phase of the outburst, where the illuminated area is larger, and thus a larger fraction of the NS atmosphere contributes to the line formation, as illustrated in Fig. 8. We note that such change indicates a significant change in the emission region structure, regardless of the assumed model for the CRSF formation.

3.2 The critical luminosity

At high luminosities, the CRSF centroid energy in V 0332+53 is known to be anticorrelated with flux, which is consistent with Cusumano et al. (2016) findings and our results for the declining phase of the outburst. However, the anticorrelation seems to break

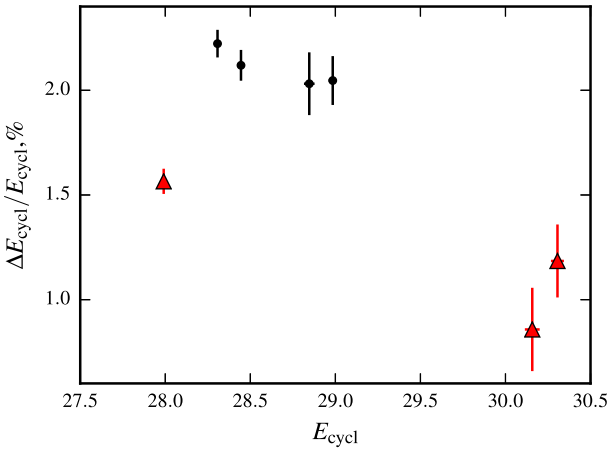

Figure 8. Amplitude of the variation of the fundamental centroid energy with pulse phase for the declining part of the main outburst (black points) and for the rest of the data (red triangles).

at the lowest flux (see Fig. 4). Indeed, the centroid energy is well constrained in the last two *NuSTAR* observations in 2015, and is actually slightly lower during the dimmer observation. A comparison of the observed line energies in two dimmest observations in 2015 thus implies a positive correlation with luminosity with $\mathrm{d}E/\mathrm{d}L = 0.16(8)$ keV/10^{37} erg s^{-1}. For the two observations in 2016, one can deduce $\mathrm{d}E/\mathrm{d}L = 1.3(7)$ keV/10^{37} erg s^{-1}, i.e. in four out of seven *NuSTAR* observations, the line energy seems to increase with flux, i.e. the anticorrelation reported for higher fluxes does not seem to extend to low fluxes indefinitely. Transition from an anticorrelation to a correlation is, in fact, expected from a theoretical point of view. The anticorrelation observed at high fluxes is thought to be associated with the change of height of the accretion column, which is supported by radiative pressure and thus appears only above a certain critical luminosity (Basko & Sunyaev 1976). Below the critical flux the line is expected to be correlated with the flux either due to the Doppler effect (Mushtukov et al. 2015c) or due to a change of the atmosphere height above the NS surface driven by ram pressure of the infalling material (Staubert et al. 2007).

Assuming that such a transition does, indeed, take place, the transitional luminosity can be estimated by fitting a broken linear model to *NuSTAR* and BAT data corrected for the linear drift, as shown in Fig. 9. This yields $L_{\rm crit} = 0.7^{+0.7}_{-0.1} \times 10^{37}$ erg s^{-1} with $E_{\rm cycl} = 30.58(7) - 0.144(4)(L - L_{\rm crit})/10^{37}$ above the transitional luminosity, and $E_{\rm cycl} = 30.58(7) + 1.4(1.2)(L - L_{\rm crit})/10^{37}$ below it. Here, we additionally include in quadrature a systematic uncertainty of 0.1 keV for BAT[2] and of 0.077 keV for *NuSTAR* to get a statistically acceptable fit [in the latter case, the systematics correspond to the uncertainty of energy scale around the mean CRSF energy assuming the long-term gain variations reported by Madsen et al. (2015)]. The best-fitting statistics improve from $\chi^2_{\rm red} = 1.37$ for 27 degrees of freedom for a linear fit to $\chi^2_{\rm red} = 1.03$ for 25 degrees of freedom for the broken linear fit, which implies that the latter model is marginally preferred at an $\sim 3\sigma$ confidence based on the MLR test (Protassov et al. 2002). Note that while the transitional luminosity value seems to be in good agreement with theoretical predictions, as illustrated in Fig. 10, both the significance level and the deduced parameters might be affected by the assumptions that

[2] http://heasarc.nasa.gov/docs/heasarc/caldb/swift/docs/bat/SWIFT-BAT-CALDB-ESCALE-v1.pdf

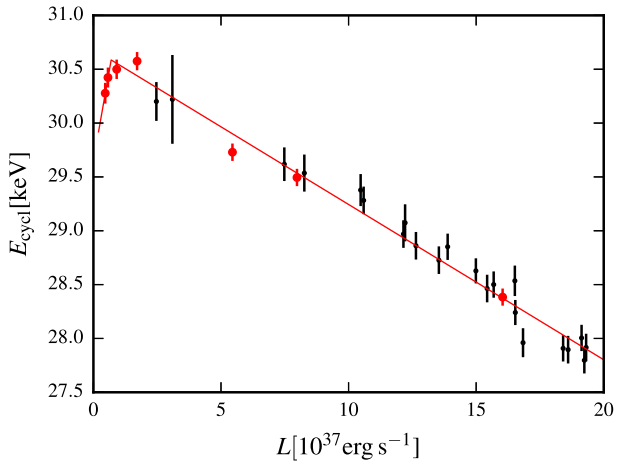

Figure 9. Correlation of the CRSF centroid energy on luminosity with the linear drift of $\dot{E}_{cycl} = -0.015$ keV d^{-1} taken into account (symbols are the same as in Fig. 4). Note the transition from anticorrelation to correlation below 10^{37}erg s^{-1}.

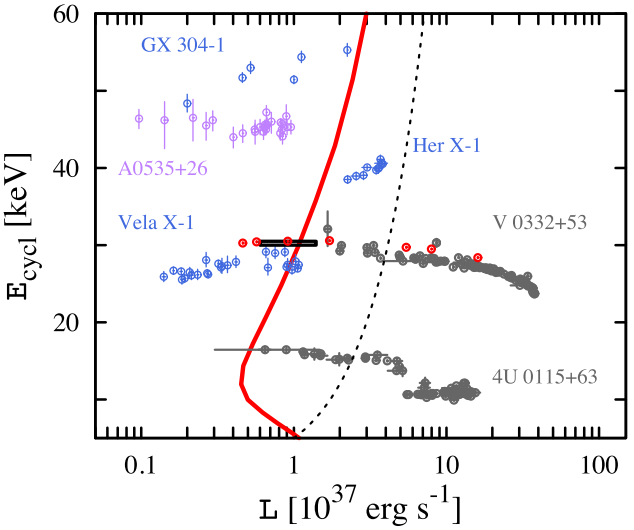

Figure 10. CRSF energy as a function of luminosity for sources where either a correlation or an anticorrelation was reported in the literature. The red circles correspond to *NuSTAR* data reported in this work. The black box corresponds to the estimated value of the transitional luminosity. The red solid curve corresponds to the critical luminosity value (Mushtukov et al. 2015a) for the case of $\Lambda = 0.5$, where Λ is the ratio of magnetospheric radius to Alfvén radius, and the radiation dominated by *X*-mode polarization.

the line energy decreased linearly during the giant outburst and has fully recovered between the two outbursts.

On the other hand, the slope of the anticorrelation at high fluxes, which shall be less sensitive to either assumption, is in good agreement with value reported by Tsygankov et al. (2010), i.e. seems to be robustly constrained. We can, therefore, compare it with slopes deduced for the low flux observations, as reported above, which implies a deviation of $\sim 3.5\sigma$ and $\sim 2\sigma$ for 2015 and 2016 observations, respectively. Here, we include no systematical uncertainties as the *NuSTAR* gain is expected to remain stable on short time-scales. One can also estimate the correlation slope at low luminosities by fitting all four low-flux observations with a linear model with a common slope and arbitrary intercepts for 2015 and 2016 low-flux observations. This allows us to account for the possibility that the line energy has not completely recovered between the outburst, as well as for possible long-term energy scale variations. The corresponding best-fit $dE/dL = 0.17(8)$ keV/10^{37} erg s^{-1} and deviates by $\sim 3.8\sigma$ from value obtained for higher fluxes.

We conclude, therefore, that *NuSTAR* data provide a first hint of the transition from anticorrelation to correlation of the CRSF energy with flux at low fluxes. As illustrated in Fig. 10, the transitional luminosity is in agreement with theoretical predictions for the onset of an accretion column, so it is natural to associate the change in correlation slope with the disappearance of the accretion column. On the other hand, a comparatively low statistical significance of the correlation break together with the complex evolution of line energy throughout the giant outburst and between the 2015 and 2016 outbursts makes it hard to justify whether the transition is, indeed, robustly detected, so additional observations are required to confirm our findings.

3.3 The 'mini'-outburst in 2016

Finally, we would like to comment briefly on the *Swift*/XRT light curve of the source in 2016 July–August. Traditionally, outbursts of Be-transients are classified into two types, i.e. 'giant' ones like that observed from V 0332+53 in 2005 and 2015, and 'normal' ones that typically occur at periastron and are detectable with all-sky monitors like *Swift*/BAT. Both burst types are evident in the long-term V 0332+53 light curve. However, a closer inspection also reveals some flux enhancements at almost every periastron with a level below that typical for 'normal' outbursts. This prompted us to request additional *NuSTAR* observations and *Swift*/XRT monitoring, which, indeed, revealed a minor outburst with peak luminosity $\sim 6 \times 10^{36}$ erg s^{-1} barely detectable also by BAT. We note that even lower level accretion can occur in V 0332+53 and other Be-transients also when they are not detected by all-sky monitors, and this might have important consequences for studies dedicated to the cooling of the NSs (Wijnands & Degenaar 2016).

The light curve itself is also quite interesting as it reveals a sharp dip in the vicinity of the periastron. A similar behaviour was reported recently by Ferrigno et al. (2016) during the 2015 giant outburst. They interpreted the observed orbital modulation as flux enhancement following the periastron passage associated with the accretion of matter captured at periastron and delayed by the propagation through the accretion disc. In our case, it is, however, clear that the outburst starts before the periastron and the accretion rate drops for ~ 3 d to restore later to the pre-dip level (see Fig. 2). We note that the light-curve modelling by Ferrigno et al. (2016) is not unambiguous, and the observed modulation during the giant outburst can also be attributed to the dips at periastron rather than flux enhancement afterwards. We conclude, therefore, that taking into account our findings, the interpretation or orbital modulation suggested by Ferrigno et al. (2016) is probably not correct. On the other hand, the observed flux drop at periastron is at odds with the commonly accepted picture of outbursts in Be-transients, which are believed to be triggered by the enhanced accretion as the NS passes through the disc of the primary close to the periastron.

A complex outburst development has been reported also for other Be-systems (Postnov et al. 2008; Klochkov et al. 2011). For 1A 0535+262, Postnov et al. (2008) attributed the initial flare to unstable accretion triggered by some magnetospheric instability, and the following dip to the depletion of the inner disc regions. In the case of V 0332+53, however, a similar behaviour was also observed during the outburst at high accretion rates, which makes this explanation unlikely. The dip in V 0332+53 is also clearly not

related to enhanced absorption as the ratio of XRT/BAT fluxes remains constant. We hesitate to provide a better explanation, and a discussion of the physical origin of dips is out of the scope of this paper. Still, we wanted to bring this issue up to illustrate that the exploration of the properties of the Be-transients at low luminosities enabled for the first time by *NuSTAR* and *Swift*/XRT is very interesting, indeed, and shall be continued.

4 CONCLUSIONS

Based on the analysis of *NuSTAR* observations of V 0332+53 during the declining part of the 2015 giant outburst, we have confirmed the previously known anticorrelation of CRSF energy with luminosity. We also confirm the apparent drop of the CRSF centroid energy during the declining part, recently interpreted by Cusumano et al. (2016), as the result of the accretion-induced decay of the magnetic field of the NS. We find that the line energy decrease is consistent with being time linear throughout the outburst with a rate of $\sim$0.015 keV d^{-1}. Furthermore, follow-up *NuSTAR* observations of another outburst in 2016 revealed that the line energy has increased again approximately to values observed before the 2015 outburst which implies a recovery rate of $\sim$0.05 keV d^{-1}. Both time-scales imply an unprecedentedly fast evolution of the magnetic field of the NS if the change of the observed line energy is directly related to field strength, as suggested by Cusumano et al. (2016). We argue, however, that the evolution of the observed CRSF energy is likely, instead, associated with a change of the emission region geometry. The latter is defined by the magnetosphere size, which, indeed, seems to be different in rising and declining parts of the outburst, as suggested by the observed spin evolution of the NS.

Finally, we find that at luminosities below $\sim 10^{37}$ erg s^{-1} the anticorrelation of the CRSF energy with flux reported for higher luminosities seems to break, which we interpret as the first observational evidence for the transition from super- to sub-critical accretion. The transitional luminosity is in agreement with the theoretical predictions and cyclotron line luminosity dependence observed in other sources, as shown in Fig. 10. We note, however, that taking into account the complex evolution of line energy throughout the outburst and a comparatively low statistical significance of the break, the transition cannot be considered to be robustly detected, and additional observations are required to confirm our findings.

ACKNOWLEDGEMENTS

Authors thank E. M. Churazov, who developed the *INTEGRAL*/SPI data analysis methods and provided the software. This research has made use of data provided by HEASARC (NASA/GSFC and Smithsonian Astrophysical Observatory). This work is based on observations with *INTEGRAL*, an ESA project with instruments and a science data centre funded by ESA member states (especially the PI countries: Denmark, France, Germany, Italy, Switzerland and Spain), and with the participation of Russia and the USA. This work made use of data supplied by the UK Swift Science Data Centre at the University of Leicester. The authors acknowledge support from the Deutsches Zentrum für Luft- und Raumfahrt (DLR) through DLR-PT grant 50 OR 0702 (VD), Deutsche Forschungsgemeinschaft (DFG) through WE 1312/48-1 (VFS), the Russian Science Foundation through grant 14-12-01287 (AAM, SST and AAL), the Academy of Finland through grant 268740 and the Foundations' Professor Pool, the Finnish Cultural Foundation (JP).

REFERENCES

Basko M. M., Sunyaev R. A., 1976, MNRAS, 175, 395
Becker P. A. et al., 2012, A&A, 544, A123
Choudhuri A. R., Konar S., 2002, MNRAS, 332, 933
Churazov E., Sazonov S., Tsygankov S., Sunyaev R., Varshalovich D., 2011, MNRAS, 411, 1727
Churazov E. et al., 2014, Nature, 512, 406
Cusumano G., La Parola V., D'Aì A., Segreto A., Tagliaferri G., Barthelmy S. D., Gehrels N., 2016, MNRAS, 460, L99
Doroshenko V., Tsygankov S., Santangelo A., 2016, A&A, 589, A72
Evans P. A. et al., 2009, MNRAS, 397, 1177
Ferrigno C. et al., 2016, A&A, 595, A17
Fürst F. et al., 2013, ApJ, 779, 69
Gehrels N., 1986, ApJ, 303, 336
Ghosh P., Lamb F. K., 1979, ApJ, 234, 296
Klochkov D., Ferrigno C., Santangelo A., Staubert R., Kretschmar P., Caballero I., Postnov K., Wilson-Hodge C. A., 2011, A&A, 536, L8
Klochkov D. et al., 2012, A&A, 542, L28
Klochkov D., Staubert R., Postnov K., Wilms J., Rothschild R. E., Santangelo A., 2015, A&A, 578, A88
La Parola V., Cusumano G., Segreto A., D'Aì A., 2016, MNRAS, 463, 185
Lipunov V. M., 1982a, Ap&SS, 82, 343
Lipunov V. M., 1982b, Ap&SS, 85, 451
Lipunov V. M., Semenov E. S., Shakura N. I., 1981, Soviet Astron., 25, 439
Lutovinov A. A., Tsygankov S. S., Suleimanov V. F., Mushtukov A. A., Doroshenko V., Nagirner D. I., Poutanen J., 2015, MNRAS, 448, 2175
Madsen K. K. et al., 2015, ApJ, 801, 66
Mihara T., Makishima K., Ohashi T., Sakao T., Tashiro M., 1990, Nature, 346, 250
Mushtukov A. A., Suleimanov V. F., Tsygankov S. S., Poutanen J., 2015a, MNRAS, 447, 1847
Mushtukov A. A., Suleimanov V. F., Tsygankov S. S., Poutanen J., 2015b, MNRAS, 454, 2539
Mushtukov A. A., Tsygankov S. S., Serber A. V., Suleimanov V. F., Poutanen J., 2015c, MNRAS, 454, 2714
Mushtukov A. A., Nagirner D. I., Poutanen J., 2016, Phys. Rev. D, 93, 105003
Nakajima M., Mihara T., Makishima K., 2010, ApJ, 710, 1755
Postnov K., Staubert R., Santangelo A., Klochkov D., Kretschmar P., Caballero I., 2008, A&A, 480, L21
Pottschmidt K. et al., 2005, ApJ, 634, L97
Poutanen J., Mushtukov A. A., Suleimanov V. F., Tsygankov S. S., Nagirner D. I., Doroshenko V., Lutovinov A. A., 2013, ApJ, 777, 115
Protassov R., van Dyk D. A., Connors A., Kashyap V. L., Siemiginowska A., 2002, ApJ, 571, 545
Rappaport S., Joss P. C., 1977, Nature, 266, 683
Santangelo A. et al., 1999, ApJ, 523, L85
Staubert R., Shakura N. I., Postnov K., Wilms J., Rothschild R. E., Coburn W., Rodina L., Klochkov D., 2007, A&A, 465, L25
Staubert R., Klochkov D., Vybornov V., Wilms J., Harrison F. A., 2016, A&A, 590, A91
Titarchuk L., 1994, ApJ, 434, 570
Tsygankov S. S., Lutovinov A. A., Churazov E. M., Sunyaev R. A., 2006, MNRAS, 371, 19
Tsygankov S. S., Lutovinov A. A., Serber A. V., 2010, MNRAS, 401, 1628
Tsygankov S. S., Lutovinov A. A., Doroshenko V., Mushtukov A. A., Suleimanov V., Poutanen J., 2016, A&A, 593, A16
Wang Y.-M., 1987, A&A, 183, 257
Wijnands R., Degenaar N., 2016, MNRAS, 463, L46

This paper has been typeset from a TEX/LATEX file prepared by the author.